Available online at www.sciencedirect.com
SCIENCE DIRECT®
ELSEVIER
International Journal of Solids and Structures 42 (2005) 4859–4879
INTERNATIONAL JOURNAL OF SOLIDS and STRUCTURES
www.elsevier.com/locate/ijsolstr

Path dependency in hybrid structures with simultaneous ductile and brittle connections and materials

Wendel Michael Sebastian *

Department of Civil Engineering, University of Bristol, Queen's Building, University Walk, Bristol BS8 1TR, UK

Received 3 September 2003; received in revised form 22 January 2005
Available online 16 March 2005

Abstract

This article considers a steel–stud–concrete hybrid structure with a Fibre Reinforced Polymer plate adhesively-bonded to the steel member. Owing to the combination of ductile and brittle materials and connections present, the failure behavior of such a structure can be influenced by residual stresses, which in turn depend on the plasticity-inducing load paths previously experienced by the structure. Plasticity of only the stud connections generates a different residual stress pattern from plasticity of only the steel member, and an understanding of the mechanics of residual stress generation in each case is fundamental to the development of a framework of ideas on path dependency in such structures. Measurements of deformation do not necessarily permit faithful reconstruction of residual stress profiles, as these measurements typically give *total* (elastic plus plastic) deformations from the times that the measurements start, while the residual stresses are related to the *elastic* components of deformation from the times that the structural components were manufactured. *Numerical* work is thus needed to determine residual stresses. To that end, a verified finite element program is here used to investigate residual stress patterns in the above hybrid structure due to plasticity of either the studs or the steel member. For yield of the steel, the effects on the residual stresses of initial self-equilibrating stresses in the steel member are investigated. Crucial to the success of the analyses are curvilinear or multi-linear loading/unloading constitutive relationships not only for the materials, but also for the connections. The residual stress profiles from the steel yield and stud yield analyses are examined and compared, and ideas for extension of the work are suggested.

Keywords: Ductile; Brittle; Connection; Adhesive; Stud; Path dependency; Residual stresses; Hybrid

* Tel.: +44 117 928 9735; fax: +44 117 928 7783.
E-mail addresses: wheels1541@hotmail.com, wendel.sebastian@bristol.ac.uk

0020-7683/$ - see front matter
doi:10.1016/j.ijsolstr.2005.01.017

1. Introduction

Structural rehabilitation and repair using adhesively-bonded Fibre Reinforced Polymers (FRP) has been investigated extensively for *concrete* structures (Varastehpour and Hamelin, 1996; Burgoyne, 2001; Sebastian, 2001, 2002a,b) and, to a much lesser extent, for structural steel members (Mertz and Gillespie, 1996; Sebastian, 2003a). Application of this plate bonding technology to structural steel–concrete slab hybrid members is the logical next step. This new application is illustrated in Fig. 1, from which it is seen that the uni-directional FRP plate acts as tension reinforcement to the steel member. Stress transfer between the FRP plate and the steel member through the adhesive connection, and also between the concrete slab and the steel member through the stud connections, permit development of hybrid structural action.

One key facet of this hybrid structural form is the mixture of ductile and brittle materials and connections present. Into the ductile category fall the stud connections and steel material, while the brittle category includes the FRP material and adhesive connection. The concrete material is also brittle. Even if there is prior plastic deformation of the ductile components, failure of the structure can well be brittle, because such failure can occur through either the adhesive connection, the concrete, or also potentially through the FRP.

Failure of the brittle components can be influenced by, among other factors, residual stresses present in the structure. The nature of this influence depends not only on the magnitudes of the residual stresses at the critical locations, but also on the signs of these residual stresses relative to the signs of the additional stresses generated by the failure load. Changes to the spatial distribution of residual stresses in the structure may induce *migration* of the critical failure location. Even if there are zero residual stresses at the critical locations, non-zero residual stresses in the ductile parts of the structure may have been sufficient to yield those parts before the failure load is applied. In such cases, during the final loading event, the distribution of stiffness within the structure, and so the rate of change with load of stresses at the critical locations, can be influenced by the sizes and locations of these pre-yielded regions. Hence residual stresses can influence

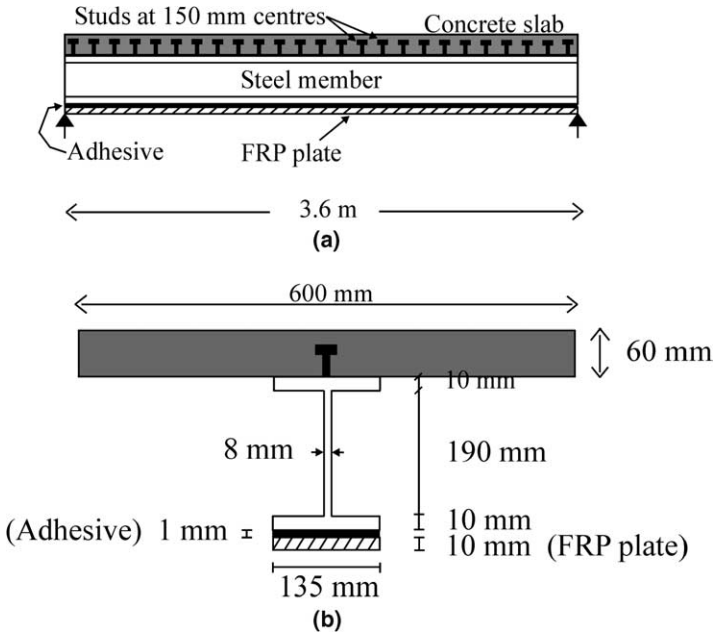

Fig. 1. Steel–concrete composite member with adhesively-bonded FRP plate. (a) Studs and (b) steel and FRP.

failure even when these stresses are zero at the critical locations. As discussed below, the magnitudes and spatial distribution of these residual stresses depend on the load paths which define the structure's history. The objective of the present paper is to identify fundamental characteristics of the residual stress patterns through which this *path dependency* becomes manifest.

Ironically, although the *final failure* can commonly occur through *brittle* parts of the structure, the *residual stresses* which influence this failure typically arise from the actions of the *ductile* parts of the structure. The residual stresses, which increment with each yield-inducing load pass, develop because the loading and unloading constitutive relationships for a typical ductile component are not identical when plastic deformation occurs during loading; see Fig. 2. The post-plastic unloading line is typically elastic. After application and removal of external loading, the elastic and plastically-deformed parts of the structure will not all have traveled along their loading–unloading characteristics to the same extent, so a self-equilibrating system of internal stresses develops in the final unloaded configuration of the structure. A plastically-deformed part may end up either in a reverse-loaded residual state or in a forward-loaded residual state, see Fig. 2.

Residual stresses can exist in the individual structural components even before the entire structure is fully assembled. For example, differential cooling rates after both the hot-rolling manufacturing process and welding of the studs can induce residual stresses in the steel member. Since measurements of strain and slip are usually made *after* assembly of the entire structure, these original residual stresses are not quantified. Further, in a real structure, measurements of deformation will typically be taken only after the structure is deemed to be suspect, by which time plasticity-inducing loads may have already been experienced. Residual effects from these earlier loads will not be captured by the tardy measurements. In addition, while residual stresses depend only on the *elastic* components of deformation, many conventional methods of measurement capture the *total* deformations, which include both the elastic and plastic components; themselves not easily separated. It thus seems sensible to complement measurement of deformations with advanced nonlinear analytical work, as this will permit representative quantification of residual stresses as long as both the external actions on, and the constitutive relations for, the components of the structure can be modeled.

Studs are *discrete*, and yield of the studs progresses *along* the span of the member. By contrast, the steel member is *continuous* in space, and yield of the steel progresses both *along* and *normal* to the span of the member. Also, yield of the studs initiates in zones of high *shear force*, while yield of the steel starts in zones of high *moment*, and the zones of high shear and high moment do not necessarily coincide. These differences suggest that yield of the studs may well generate a different residual stress profile in the structure from yield of the steel member. A fundamental appreciation of these different profiles is

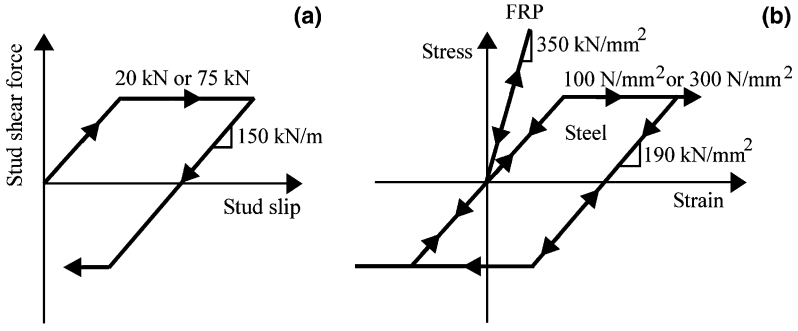

Fig. 2. Loading–unloading characteristics of studs and materials. (a) Studs and (b) steel and FRP.

an essential first step in understanding the complex response of this structural form to varying sequences of external loading.

In a research environment, a firm appreciation of residual stress patterns is useful for at least two reasons. First, it is important for dealing with lab specimens which experience pragmatic unloading (due to, say, valve rupture or exhaustion of the travel in a hydraulic loading jack) during their first excursions into the elasto-plastic regime. For subsequent re-loading, knowledge of the residual stress pattern is crucial to a proper analysis of the failure behavior. Second, it commonly occurs that, owing to resource limitations, a given laboratory specimen is sequentially loaded into its elasto-plastic regime under different external actions. This process extracts large banks of information on structural behavior, while minimizing consumption. Clearly, quantification of the residual stress build-up is crucial if the results are to be correctly interpreted. In practice, an understanding of the mechanics of residual stress generation is useful when the following considerations are taken into account:

- *Shakedown or ratcheting*. The structure may experience *plastic* shakedown, whereby self-neutralizing plastic strains develop within each load cycle, so that there is zero net permanent deformation when loading ceases. This can lead to low-cycle fatigue failure of the plastically-deforming parts, particularly the stud connections. Alternatively, *elastic* shakedown may occur where, after accruing permanent deformations and stresses within the first few cycles, the structure with locked-in residual stresses exhibits solely elastic response to subsequent loads. A third possibility, that known as ratcheting, is the monotonic accumulation of permanent deformation, and so of residual stress, after each plasticity-inducing load event.
- *Fatigue of adhesive and studs*. In bridges, long-term residual actions on the adhesive and studs can reduce the tolerance of these components to high-cycle fatigue from traffic loading.
- *Thermal stresses in the adhesive*. Owing to the significant disparity in coefficient of thermal expansion between FRPs and steel, temperature changes in this hybrid structure can generate high stresses in the adhesive connection. These thermal stresses can be significant, and residual stresses in the adhesive can alter the tolerance of the structure to this thermal effect.
- *Replacement of the plates*. FRP delamination and/or suspect bond may require that the plates on an in-service structure be replaced. Residual stresses lock elastic potential energy into both the plates and the adhesive, and this energy will be released on removal of the plates. This has important safety implications for the design of the plate removal scheme.
- *Post-seismic serviceability*. Earthquake loading on a building can induce complex residual stress states in this structural form. The structure's ability to perform its normal load-bearing function afterwards can be strongly influenced by these seismically-induced residual stresses.
- *Risk assessment*. The loads generating residual stresses in a structure are not always accurately quantifiable. Risk assessment is now used to allow for the uncertainties, and basic to such assessment is reliable quantification of residual effects under pre-defined loads.

In the rest of this paper, the residual stresses in a FRP–adhesive–steel–stud–concrete hybrid structure under one pass of uniformly distributed loading are determined using nonlinear finite element (FE) analysis. Three different FE analyses are conducted; one in which yielding occurs in the stud connections but not in the steel beam, and two others in which yielding occurs in the steel beam but not in the studs. Of the latter two, one analysis assumes zero initial stress in the steel member, while the other employs an initial stress state in the steel member from, say, a hot-rolling manufacturing process. The material models, FE program and considered specimen are described in the next section. Results are then presented and discussed, avenues still open for further work are put forward, and conclusions are drawn. Note that the terms *nonlinear* and *curvilinear* are used interchangeably below.

2. Model definition

2.1. Constitutive relations

A 3-D curvilinear constitutive model is adopted for the concrete, which possesses a uni-axial compressive strength of 20 N/mm^2, along with the following properties in the undeformed state: Young's Modulus of 27.1 kN/mm^2, Poisson's ratio of 0.15, hence shear modulus of 11.8 kN/mm^2. The form of the constitutive model depends on the sign of the average principal strain. If the principal strains are ε_1, ε_2 and ε_3 with ε_1 and ε_2 being in the plane of the slab while ε_3 is normal to this plane, the average principal strain is as follows:

$$\varepsilon_a = \frac{(\varepsilon_1 + \varepsilon_2 + \varepsilon_3)}{3}. \tag{1}$$

When this strain is tensile and the concrete is uncracked, the material moduli and Poisson's ratio assume the undeformed values. If, instead, this average strain is compressive, then these moduli change with the level of deformation. In establishing these deformed moduli in compression, the octahedral shear strain, defined as follows, must first be determined

$$\gamma_o = \frac{2}{3}\sqrt{(\varepsilon_1 - \varepsilon_2)^2 + (\varepsilon_2 - \varepsilon_3)^2 + (\varepsilon_3 - \varepsilon_1)^2}. \tag{2}$$

The secant bulk modulus, K_s, and secant shear modulus, G_s, for this deformed state are then

$$K_s = K_u(0.85 \times 2.5^{-714\varepsilon_a} + 0.15), \tag{3}$$

$$G_s = G_u(0.81 \times 2^{-500\gamma_o} - 2\gamma_o + 0.19), \tag{4}$$

where K_u and G_u are the undeformed bulk and shear modulus respectively. The present FE analysis assumes a 2-D stress state in the plane of the concrete slab, so through-thickness direct stresses in the slab are ignored. This leads to the following useful simplification

$$\varepsilon_3 = -\upsilon_s \frac{(\varepsilon_1 + \varepsilon_2)}{(1 - \upsilon_s)}, \tag{5}$$

where υ_s is the secant Poisson's ratio in the deformed state. Once K_s and G_s have been determined, υ_s may be established as follows:

$$\upsilon_s = \frac{(3K_s - 2G_s)}{2(3K_s + G_s)}. \tag{6}$$

Perusal of Eqs. (1)–(6) shows that parameters ε_a, ε_3, υ_s, G_s and K_s are inter-dependent, and a local iterative process is used in the FE program to establish the updated moduli once ε_1 and ε_2 are known. This local iterative process uses, as starting values, the stored local secant moduli from the previous load iteration. Once these deformed shear and bulk moduli are known, the deformed Young's modulus, E_s, is obtained as follows:

$$E_s = \frac{9G_sK_s}{3K_s + G_s}. \tag{7}$$

These concrete constitutive models, implemented in the present FE program, have led to predictions of structural response in good agreement with test data (Sebastian and McConnel, 2000).

In the present analyses, by far the dominant strain in the slab is that along the span of the steel member. Therefore, in these analyses, concrete compression failure is deemed to occur at any Gaussian integration point of any concrete finite element if the longitudinal strain at that point is compressive and equals the

concrete uni-axial failure strain of 0.0035. Also in these analyses, the compression concrete does not extend very far into the curvilinear regime, so the loading and unloading behaviors of the compression concrete are taken to be identical to each other. Further, the FE results also show that only small tensile stresses develop at the soffit of the concrete slab, so no cracking of the concrete is assumed. Instead, linear behavior along identical loading and unloading lines is assumed for tension concrete.

Fig. 2 shows that the stud connections and the steel material are assumed to exhibit elastic–perfectly plastic behavior with zero Bauschinger effect for load reversal. Also, the loading and unloading lines are assumed to be parallel for each of these components (Fig. 2). Either of two yield shear forces (studs) or two yield axial stresses (steel) is used depending on whether yield of only the studs or only the steel is required in the FE analysis. The steel is of Young's modulus 190 kN/mm^2 and yield stress of either 100 N/mm^2 or 300 N/mm^2. The studs possess an elastic (shear force vs slip) modulus of 150 kN/mm and a yield shear force of either 20 kN or 75 kN. Uplift on the studs is assumed to be sufficiently small as not to affect shear yield strength. In practice, stud connections show a curvilinear behavior (Yam and Chapman, 1972) which is well approximated by Fig. 2.

Quasi-static loading is assumed, so properties at zero strain-rate apply to the adhesive. Hence the adhesive is assumed to be linear elastic, with Young's and shear moduli of 1.4 kN/mm^2 and 0.5 kN/mm^2 respectively. An ultra-high modulus FRP, of Young's modulus 350 kN/mm^2, is also assumed (Fig. 2). The peak axial stress in the FRP from all the FE analyses is well below the assumed FRP failure stress of 1000 N/mm^2, so tensile rupture of the FRP was not critical in any of these analyses.

In general, it is assumed that the failure deformations of all the materials and the studs exceed the corresponding peak deformations reached in the present FE analyses, and so no failure of the materials (and of the bond through the adhesive) occurs in the analyses.

2.2. Finite element program

The present nonlinear finite element (NLFE) program has successfully been used to analyse structures comprising different combinations of concrete slabs, shear studs, structural steel members, adhesives and structural FRP components (Sebastian and McConnel, 2000; Sebastian, 2003a,b). In this program, the displacement control algorithmic strategy is used for computational stability and to ensure rapid numerical convergence in nonlinear regimes of behavior.

Fig. 3(a) shows an assembly of finite elements. From symmetry considerations, only half the width of the structure is modeled. Along this plane of symmetry, the degrees-of-freedom v and θ_y are both zero. The concrete slab is represented by 4-noded elements, the steel beam and FRP plate each by 2-noded elements, and the stud and adhesive connections by special interface elements. Each discrete stud connection is modeled by one interface element, while the continuum adhesive layer is closely approximated by several interface elements along the span. Each adhesive interface element represents the full thickness of the adhesive layer. The stresses in the adhesive layer can vary between adjacent studs, so multiple adhesive elements are used between each pair of stud elements. Hence, in Fig. 3, only *two* nodes of the 4-noded slab element and only *one* stud element appear, because the FE assembly shown is that between only *two* adjacent *adhesive* elements. This explains, at the back end of the mesh of Fig. 3(a), the absence of nodes for the slab element (note the squiggle at that end of the slab element indicating continuity of the element beyond that end), and hence the absence of a stud element. Allowance for shear lag in the slab is made by using multiple elements across the width of the slab (only one element is shown across the width in Fig. 3 for clarity).

The slab, beam and plate elements all assume plane sections, and they all allow for membrane, twisting and bending actions. By evaluating the net strains as sums of membrane, flexural and torsional contributions, these elements permit *coupling* between the above actions. Further, these elements are *layered* to accommodate through-depth variations in material properties arising from vertical progression of, say, plasticity and cracking through the steel member and concrete slab. Both the stiffness matrices and the

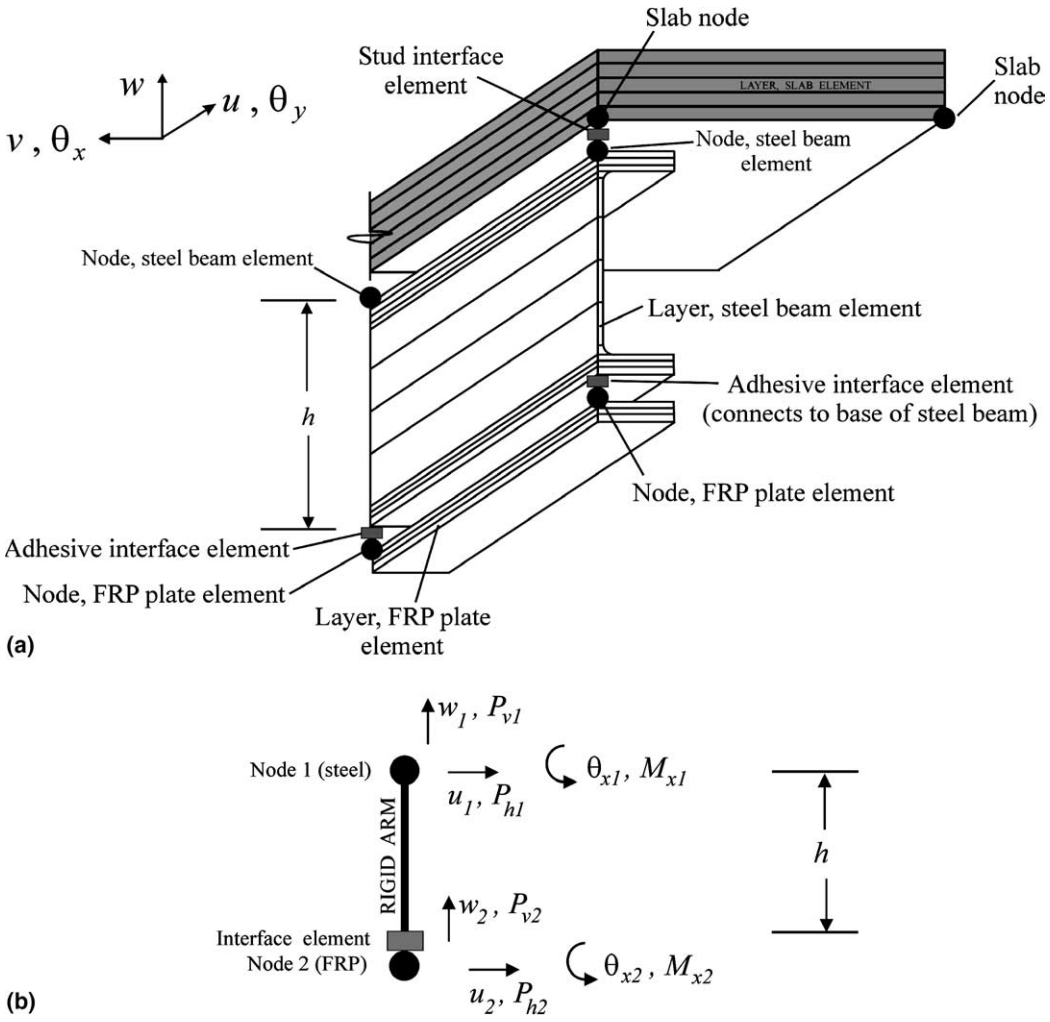

Fig. 3. Typical assembly of finite elements. (a) Assembly of elements and (b) actions of adhesive interface element.

equivalent nodal stress-resultant vectors for these elements are developed by summing the individual contributions from all the layers passing through all the Gaussian integration points within the elements. For each Gauss point, the strains and stresses calculated at the mid-thickness of each layer are taken as applying to the part of the volume of that layer associated with that Gauss point. Four Gauss points, distributed symmetrically about the centre of the element in plan, are used for the 4-noded element, while 2 Gauss points are used for the 2-noded element.

In general, each interface element comprises five springs which model resistance to separation, to slip both along and normal to the span, and to relative rotation about both horizontal axes (θ_x and θ_y in Fig. 3(a)). In the present problem, symmetry dictates that only the longitudinal slip spring, the separation spring and the rotational spring associated with degree-of-freedom θ_x are active. Within each *stud* interface element, the active separation and rotation springs are allocated large stiffnesses to enforce compatibility of the associated degrees-of-freedom between the connected slab and beam elements, while the longitudinal slip spring is allocated a secant stiffness consistent with the updated shear force and slip.

The steel nodes and adjacent concrete nodes are initially coincident, so the *stud* elements connect directly into the adjacent steel nodes. However, the steel nodes and adjacent FRP nodes are separated by the height of the steel member, and the *adhesive* elements connect first into the base of the steel member, which in turn connects to the nodes at the top of the steel member through rigid arms which rotate in harmony with those steel nodes. This situation for a typical adhesive element is clearly depicted in Fig. 3(b), where the active nodal degrees-of-freedom (u, w, θ_x) and the corresponding equivalent nodal actions (P_h, P_v, M_x) for this element are clearly illustrated. The subscripts 1 and 2 refer to the steel and FRP nodes respectively, while h is the height of the steel section as illustrated in Fig. 3(a). From Fig. 3(b) it is seen that the longitudinal displacement, u_t, of the top of the adhesive interface element is the sum of two contributions, as follows:

$$u_t = u_1 + h\theta_{x1}, \tag{8}$$

while the longitudinal displacement, u_b, of the base of the adhesive interface element is

$$u_\mathrm{b} = u_2. \tag{9}$$

This gives the following expression for the longitudinal slip through the adhesive element:

$$\text{slip} = u_t - u_\mathrm{b} = u_1 + h\theta_{x1} - u_2. \tag{10}$$

Thus, owing to the vertical offset between the top of the adhesive interface element and the adjacent steel node, the longitudinal shear action of the adhesive element depends not only on the relative longitudinal translation between the steel and FRP nodes, but also on the rotation at the steel node. Another important consequence of this offset is that the longitudinal shear force at the top of the adhesive interface element is eccentric with respect to the adjacent steel node, and so this force gives not only an equivalent nodal *force* contribution, but also an equivalent nodal *moment* contribution, to that steel node. The longitudinal force (but not the moment) contribution to the FRP node is also influenced by this eccentricity effect.

The adhesive element's stiffness matrix thus contains *non-zero* off-diagonal terms which are otherwise zero for conventional interface elements (such as the stud element) where there is direct connection into the end nodes. The following parameters are required for this novel stiffness matrix of the adhesive interface element: E_a, G_a are the Young's and shear moduli of the adhesive; b_a, t_a are the width and thickness of the adhesive layer, and; $l_{1\mathrm{a}}$, $l_{2\mathrm{a}}$ are the lengths, on either side of the vertical line joining the interface element's end nodes, of the portion of adhesive (total length $l_{1\mathrm{a}} + l_{2\mathrm{a}}$) represented by the element. Using these parameters, this stiffness matrix for the adhesive element is as follows:

$$\begin{Bmatrix} P_{h1} \\ P_{v1} \\ M_{x1} \\ P_{h2} \\ P_{v2} \\ M_{x2} \end{Bmatrix} = \begin{bmatrix} k_1 & 0 & hk_1 & -k_1 & 0 & 0 \\ 0 & k_2 & 0 & 0 & -k_2 & 0 \\ hk_1 & 0 & k_3 + h^2k_1 & -hk_1 & 0 & -k_3 \\ -k_1 & 0 & -hk_1 & k_1 & 0 & 0 \\ 0 & -k_2 & 0 & 0 & k_2 & 0 \\ 0 & 0 & -k_3 & 0 & 0 & k_3 \end{bmatrix} \begin{Bmatrix} u_1 \\ w_1 \\ \theta_{x1} \\ u_2 \\ w_2 \\ \theta_{x2} \end{Bmatrix}, \tag{11}$$

where h is defined in Fig. 3(b), while the stiffness coefficients k_1, k_2 and k_3 are as follows:

$$k_1 = G_\mathrm{a} b_\mathrm{a} (l_{1a} + l_{2a})/t_\mathrm{a}, \tag{12}$$

$$k_2 = k_1 E_\mathrm{a}/G_\mathrm{a}, \tag{13}$$

$$k_3 = E_\mathrm{a} b_\mathrm{a} (l_{1a}^3 + l_{2a}^3)/3t_\mathrm{a}. \tag{14}$$

Eccentricity effects are manifest at locations 1–3, 3–1, 3–3, 3–4 and 4–3 of the stiffness matrix.

2.3. Present steel–concrete–FRP specimen

Fig. 1 shows the presently considered specimen. The steel–stud–concrete component has not been detailed in this study, but rather is based on a specimen tested by Teraskiewicz (1967). This component forms a useful base for the present work, as it was successfully analysed by the present NLFE program (Sebastian, 1996). The FRP plate is proportioned to be of similar axial stiffness to the steel tension flange under elastic conditions. This ensures that, after the steel tension flange yields, the transfer of force to the plate is significant and so leads to high shear bond stress in the adhesive. This in turn gives a clear illustration of the nature of any residual stresses in the adhesive due to steel yield. The adhesive properties relate to those encountered in practice for strengthening applications.

Half the span of the specimen was modeled for FE analysis, with one interface element per stud connection, one concrete slab element per space between adjacent stud elements and three slab elements across the half-width of the actual slab (to allow for any shear lag effects in the slab). Five equal length steel elements were used per space between adjacent stud interface elements. The FRP elements match the adjacent steel elements in length, and adhesive interface elements were used between all steel nodes and the adjacent FRP nodes (hence five adhesive elements for every stud element). Six through-depth layers were used for the slab element, while 21 layers and 10 layers were used for the steel and FRP elements respectively. The external loading was applied to the nodes of the slab element.

3. Discussion of results

3.1. Reminder of general objectives

As stated earlier, three sets of analyses were conducted on this specimen, all under uniformly distributed loading on the member. In the first analysis, the shear force capacity of each stud was set at 20 kN, while the yield stress of the steel was assumed to be 300 N/mm^2. This ensured that the studs yielded while the steel member remained elastic throughout the analysis. The studs were (reasonably) assumed to possess sufficient ductility that they did not rupture during the analysis. In the latter two analyses the stud strength was increased to 75 kN, while the steel yield stress was reduced to 100 N/mm^2, so as to obtain yield of the steel along with solely elastic behavior from the studs. Of these latter two analyses, no initial stresses were assumed in the steel member in one case, while an initial self-equilibrating axial stress state (from hot-rolling say) was used for the steel member in the other case. This latter initial stress state, shown in Fig. 4 for the midspan section of the steel member, was assumed to decrease linearly from a maximum at midspan to zero at the supports. Calculations show that the concomitant initial shear stresses in the steel member are

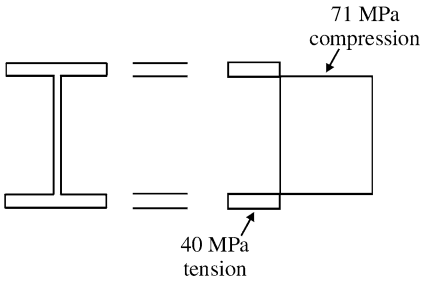

Fig. 4. Initial self-equilibrating stress state at midspan section of steel member.

small. Also, the load form used in the present analyses, namely UDL, generates low shear force and so low shear stress in the zone around midspan where steel yield occurs. For these reasons, the effects of shear stress on steel yield are ignored, and instead yield is assumed to occur when the longitudinal stress in the steel equates to the uni-axial yield stress of the steel.

The above approach ensures that residual stresses due to plasticity of the steel can be de-coupled from, and so can be compared against, residual stresses due to plasticity of the studs. In what follows, FE outputs of axial stress in the tension steel flange and FRP plate, shear forces in the studs and shear stresses in the adhesive are given for half the span (using symmetry) at the loading and residual stages. External load is per unit length of the member.

3.2. Yield of stud connections only

The uniformly distributed load on the FE model was incremented from zero to 64.7 kN/m, then back to zero. Fig. 5(a) shows the stud shear force profile along the member, from midspan to a support, for each of two load levels during the upward part of the loading cycle. The corresponding slip profiles are shown in Fig. 5(b). At the lower load level of 23.7 kN/m all studs exhibit elastic behavior, while at 64.7 kN/m, the peak load, virtually all studs are plastic. At 23.7 kN/m, except for a curved variation over a short distance near the support (an end effect), the stud force distribution (Fig. 5(a)) is linear, thereby mimicking the shear force distribution along the hybrid beam. During fully elastic behavior, the most highly loaded studs are located near the supports (Fig. 5(a)). Hence yield of the studs starts near the supports and subsequently progresses towards midspan.

The ensuing discussion focuses first on the actions of the studs per se, and then moves on to the effects of these actions on stress development in the adhesive. Fig. 6(a)–(c) qualitatively illustrate the manner in

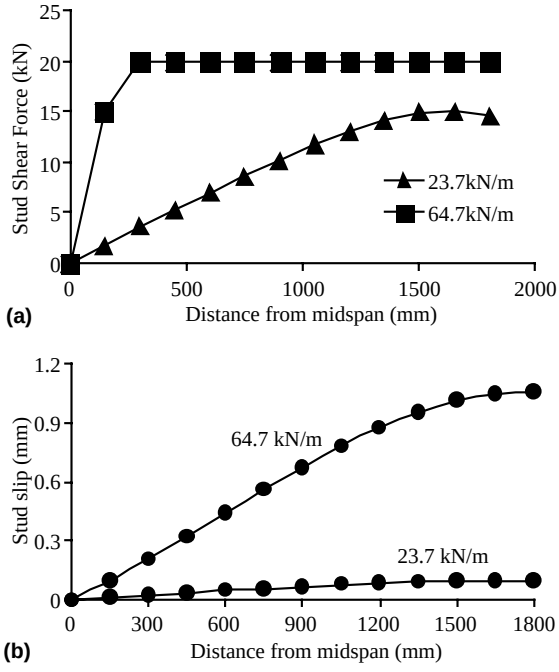

Fig. 5. Results of stud yield analysis: (a) shear force profiles along studs; (b) corresponding slip profiles.

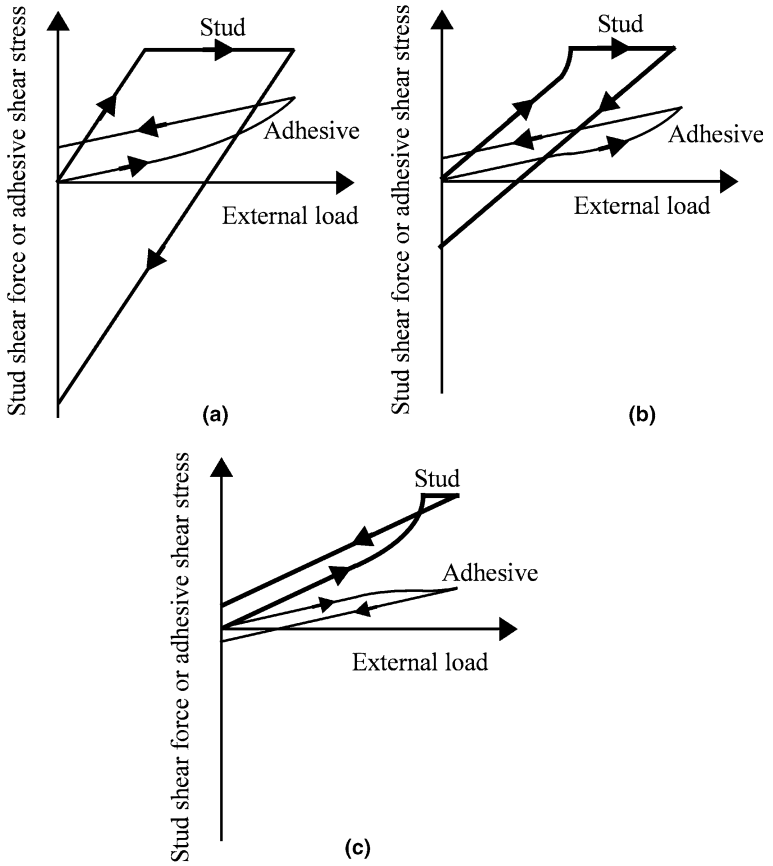

Fig. 6. Qualitative illustration of influence of stud action on adhesive shear stress: (a) no curvilinearity in stud action; (b) minor curvilinearity in stud action; (c) pronounced curvilinearity in stud action.

which stud action influences adhesive action. For the first stud to yield, and for the studs which yield subsequently, Fig. 6(a)–(c) show, in part, the anticipated variations of stud shear force with external load over the entire load cycle. In each case, the unloading line is parallel to the original elastic loading line, a fact which strongly impacts on the stud residual shear force distribution, as follows:

- For the first stud to yield, Fig. 6(a) shows that there is an initial linear increase of shear force with external load, followed by the constant shear yield force up to the peak external load, and terminated by the elastic unloading line. Due to the presence of the yield plateau after the original elastic loading line, and as the unloading line is parallel to the loading line, the path back to zero external load can only induce a *reversed* residual shear force on the stud.
- For every other stud, Fig. 6(b) and (c) show that after the initial linear regime of behavior occurs, there is a *curvilinear* change in shear force with external load *before* that stud yields, owing to the combined effect of all the other studs which have yielded beforehand. This curvilinearity takes the form of a progressive *increase* in gradient of the plot of stud shear force vs external load, because yield of the earlier-plastified studs places increased demands on the force transfer capabilities of the remaining studs which have not yet yielded.

- If the stud under consideration is near either support, then that stud will yield at a fairly low external load, and so the yield regime for that stud is quite pronounced while the above-described curvilinear regime for the stud is insignificant by comparison, see Fig. 6(b). This, coupled with the fact that the unloading line is parallel to the original loading line, dictates that the residual shear force on the stud is *reversed*, as illustrated in Fig. 6(b). Conversely, if the stud is located near midspan, then the stud will yield at a high external load, and so the curvilinear regime for that stud is significant, while the yield plateau is short. In that case, as shown in Fig. 6(c), the unloading line hits zero external load *above* the horizontal axis, which means that a *forward* residual shear force develops on the stud.
- The upshot of these mechanics is that, in proceeding from either support to midspan, the residual shear forces on the studs should change gradually from negative to positive.

Turning now to the impact of stud action on shear bond stress development in the adhesive. Together, the studs and the adhesive provide the stress transfers necessary to achieve local increase in moment along the length of the structure. Therefore, when the stud shear force increases nonlinearly upwards as in Fig. 6(b) and (c), there is less demand on the adjacent adhesive to transfer stress between the steel beam and FRP plate. In other words, the curvilinear upward *concavity* on the plot of shear force vs external load for a given stud is balanced by a curvilinear upward *convexity* on the plot of shear bond stress vs external load for the adhesive at the same section; Fig. 6(b) and (c). Conversely, when the stud travels along its yield plateau, the upper limit on axial force transfer between the concrete slab and steel beam is reached locally, and so increased demand is placed on the adjacent adhesive to transfer stress between the steel beam and FRP plate. Thus, the yield plateau on the plot of shear force vs external load for the stud triggers a curvilinear upward *concavity* on the plot of shear bond stress vs external load for the adjacent adhesive, see all of Fig. 6. Finally, recall that the adhesive material displays solely linear constitutive behavior, and so the curvilinearity in the adhesive described above is due only to the action of the nearby studs.

These mechanics dictate that, in Fig. 6(b) and (c), where the stud plots show upward *concavity* followed by the yield plateau, the adhesive shear stress vs external load plot exhibits upward *convexity* followed by upward *concavity*. Finally, recall that the unloading line for the adhesive is parallel to the loading line for the same adhesive. As a result, and as illustrated in Fig. 6(a)–(c), the residual stress in the adhesive is *forward* if the upward *concavity* is dominant, and *reversed* if the upward *convexity* is dominant. The result is that the residual shear action in the adhesive is of the opposite sign to that in the adjacent stud.

The above points are clearly borne out by the FE results presented in Figs. 7 and 8. In Fig. 7, the FE-predicted variations, with external load, of shear force on selected studs and shear stress in the adhesive adjacent to the selected studs, are plotted for the entire cycle of external load. Fig. 7(a) and (b) represent the most highly loaded stud (hence also the first stud to yield) and virtually the most highly loaded portion of adhesive respectively, both located near the supports (the studs at 150 mm from the supports and the adhesive at 180 mm from the supports), while Fig. 7(c) and (d) are for an adjacent stud–adhesive pair located at 300 mm from midspan of the structure. In addition, Fig. 8(a) and (b) show the residual shear force profile along the studs and the residual shear stress profile along the adhesive layer, respectively. These figures confirm the following ideas:

- That, for any given stud or adhesive location considered, the initial loading and final unloading lines are parallel to each other.
- That a stud which yields at low external load shows little curvilinearity before yield on the upward part of the external loading cycle and eventually experiences a reversed shear force on removal of the external load (Fig. 7(a)), while a late-yielding stud shows pronounced curvilinearity and experiences a forward residual shear force (Fig. 7(c)).

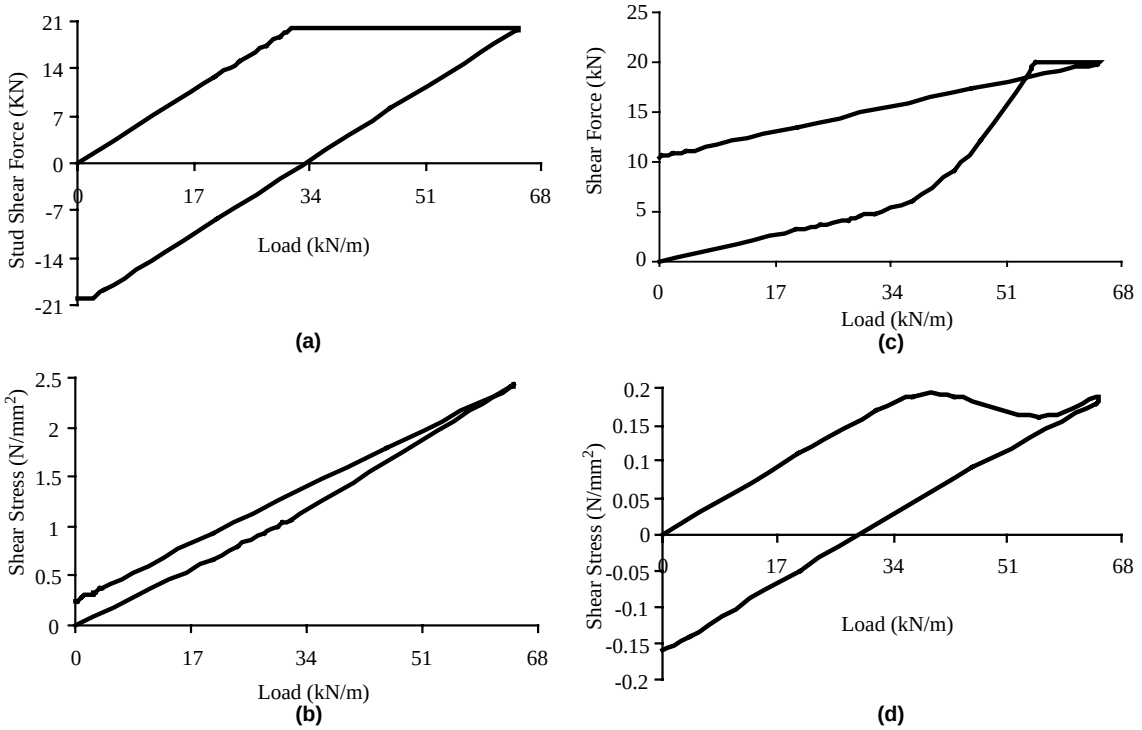

Fig. 7. Variations of stud and adhesive actions during yield of studs: (a) stud at 150 mm from support; (b) adhesive at 180 mm from support; (c) stud at 300 mm from midspan of structure; (d) adhesive at 300 mm from midspan of structure.

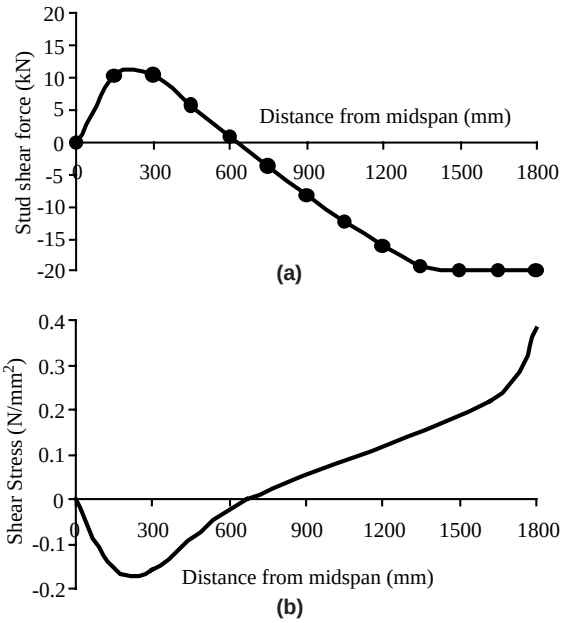

Fig. 8. Residual effects in studs and adhesive arising from yield of studs: (a) residual shear force profile along studs; (b) residual shear stress profile along adhesive layer.

- That no nonlinearity and a pronounced yield plateau for the stud (Fig. 7(a)) lead to nonlinear upward concavity and a forward residual shear stress in the adjacent adhesive (Fig. 7(b)), while extensive nonlinear upward concavity and a short yield plateau for the stud (Fig. 7(c)) give pronounced nonlinear upward convexity followed by less impacting nonlinear upward concavity and, as a result, reversed residual shear stress in the adjacent adhesive (Fig. 7(d)).
- That the residual shear force profile on the studs entails reversed loading near the supports, gradually changing to forward loading near midspan (Fig. 8(a)). In the present case, the three studs nearest the supports experience reverse yield in the residual state.
- That the residual shear stress profile in the adhesive is of the opposite sign to that in the studs (Fig. 8(b) and (a)). Also, residual yield of the studs nearest the supports has led to sharp increases of residual stress in the adhesive in those regions (Fig. 8(a) and (b)).

Fig. 7(a) shows that the most highly loaded stud yields at circa 30 kN/m load and subsequently experiences a residual shear force equal to the yield value, while Figs. 7(b) and 8(b) show a maximum shear stress of 2.4 N/mm^2 and a residual shear stress of 0.22 N/mm^2 for the adhesive locations at 180 mm from the supports.

Fig. 9 shows the residual axial stress distributions along the mid-thicknesses of the FRP plate and the tension flange of the steel member. Both sets of stresses are tensile, with a maximum of 19 N/mm^2 in the FRP plate, but only 6 N/mm^2 in the steel flange. Starting at midspan, the residual stress in the plate rises to a maximum at circa 700 mm from midspan, and then decreases to zero at the supports. Combination of the axial equilibrium and material constitutive equations for the FRP plate shows that the shear bond stress in the adhesive varies as the gradient of the axial stress at the mid-thickness of the FRP plate. By comparing the residual shear stress profile of Fig. 8(b) with the residual FRP axial stress profile of Fig. 9, it is seen that this relationship is indeed satisfied by the FE results.

The above analyses were conducted up to a maximum 64.7 kN/m external loading. In order to more clearly appreciate the nonlinear effects of stud action on adhesive action, a solely upward loading FE analysis was performed up to 98.5 kN/m UDL. Fig. 10(a) shows the corresponding shear bond stress profiles along the adhesive layer at two load levels; 20.2 kN/m, solely elastic studs, and 98.5 kN/m, advanced plasticity of the studs. The profiles of Fig. 10(a) are both nearly linear for the most part and nonlinear near the support. The sharpness of the peak near the support increases from the lower to the higher load level; further evidence of nonlinear increases of shear bond stress with load in that region. For the adhesive location at 180 mm from the support, the variation with load of shear bond stress is shown in Fig. 10(b) up to the present peak load of 98.5 kN/m UDL. A pronounced increase in gradient is observed once stud plasticity initiates. At the peak load, the tangent from the origin of the plot (see Fig. 10(b)) shows that the actual shear bond stress of 3.6 N/mm^2 is circa 12% greater than that assuming only the initial linearity from zero

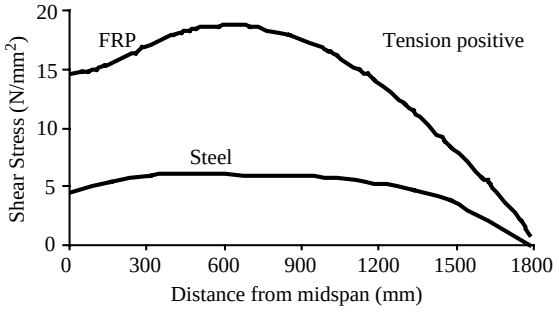

Fig. 9. Residual axial stresses in FRP plate and adjacent steel flange due to yield of studs.

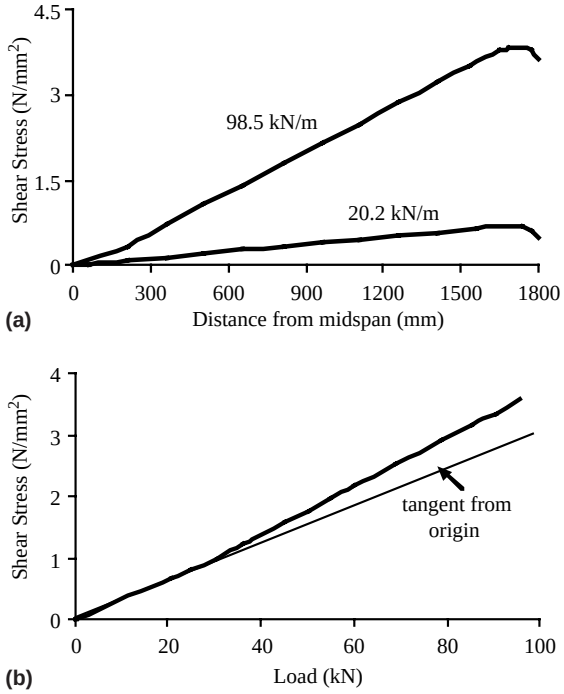

Fig. 10. Adhesive shear bond stresses during upward part of stud-yield loading cycle: (a) shear stress profile at two load levels; (b) variation with external load of shear stress at 180 mm from support.

load. Hence the nonlinear influence of stud plasticity on adhesive shear bond stress is not trivial. Care should thus be taken in using linear analysis to establish the adhesive shear stresses near the supports after the studs in that region have yielded, as this may lead to undesirable under-estimation of these adhesive stresses.

3.3. Yield of steel member only

As explained previously, two FE analyses were conducted; one in which there were no initial stresses in the steel member and also in which the UDL was incremented from zero to 98.9 kN/m and back to zero, the other in which an initial self-equilibrating axial stress distribution was assumed along the length of the steel beam and in which the UDL was taken from zero up to 95.5 kN/m and back to zero. The latter initial stress distribution, shown in Fig. 4 for the midspan cross section and decreasing linearly to zero at the supports, has peak axial tensile and compressive stresses equal to 40% and 71%, respectively, of the yield stress of the steel. In both analyses, the stud connectors were of such high yield strength (75 kN per stud) as to remain elastic throughout the cycle of external loading.

In both analyses, plasticity of the steel member started at midspan, then progressed both through the depth of, and along the length (towards the supports) of, the steel beam. When a region is elastic, significant increases of tensile stress along the member in *both* the steel and the FRP accommodate the required moment increase along the member. However, when a region becomes elasto-plastic, the yielded steel cannot sustain further increase in axial stress, and so there is significantly increased burden on axial stress from the FRP plate to sustain this moment increase along the member. Hence, with the occurrence of elasto-plasticity, the axial stress gradients along the FRP plate, and with these gradients the shear bond stresses in the

adhesive (given the relationship between shear stress and gradient of axial stress stated earlier), change dramatically and nonlinearly with applied load and with distance along the member.

Fig. 11, which shows the shear bond stress profiles between midspan and a support for two load levels, helps illustrate the point for the case with zero initial stress in the steel. At the lower load level of 59.4 kN/m, the structure is elastic, while the higher load level is the peak load of 98.9 kN/m, at which plasticity is quite advanced in the steel member. It is seen that when the structure is elastic, the shear stress profile is linear except for the curved variation very near the support. However, once plasticity of the steel occurs, the adhesive shear stress profile becomes curvilinear within the plastic zone. The higher plot of Fig. 11 shows that this curvilinearity is particularly manifest in the form of a "hump" between circa 700 mm and 1100 mm from midspan. The right side of the hump defines the outer end of the plastic zone along the steel beam. The FE output shows that this hump migrates outwards as the load increases and extends the zone of plasticity along the steel beam outwards from midspan.

For a location near the outer end of the plastic zone at peak load, Fig. 12 compares the variations of shear bond stress with external load for the cases with and without the initial stress in the steel member. On this and subsequent plots, the abbreviations NIS and WIS refer to the analytical results for No Initial Stress and With Initial Stress respectively. Fig. 12 shows that the nonlinear regime starts at a lower external load for the WIS case, owing to the earlier occurrence of steel yield when the initial stresses are present. The NIS and WIS variations have identical initial gradients, because the initial stresses make no difference to structural response while conditions remain elastic. It is also seen that the peak shear stress is larger for the WIS case, even if the peak load is slightly smaller for that case. As before, the similarity of the loading and unloading gradients for each variation, coupled with the largely upward concave nature of the nonlinear variations,

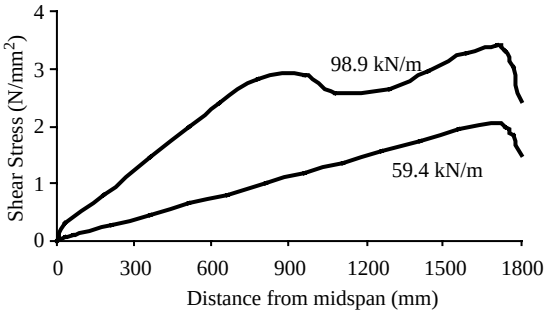

Fig. 11. Adhesive shear stress profiles for steel yield analysis with no initial stress.

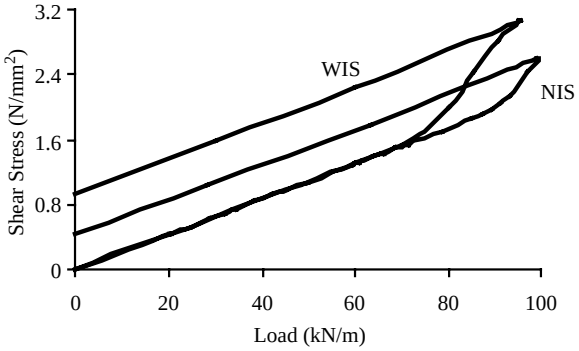

Fig. 12. Effect of initial steel stress on adhesive shear stress variation at 1080 mm from midspan.

dictates that the residual shear stress is forward rather than reverse. Moreover, owing to the earlier onset of nonlinear behavior for the WIS plot, the residual shear stress is larger for this case than for the NIS case.

The above arguments apply equally throughout the elasto-plastic regime, and so it may be anticipated that the residual shear bond stresses in the regions which experienced elasto-plastic behavior would possess two main characteristics. First, these stresses are wholly forward (never reversed), and second, they are significant further out from midspan for the WIS case than for the NIS case. In the regions near the supports where the steel does not yield, only negligible residual shear bond stresses would be encountered. Fig. 13 confirms these ideas.

Fig. 14(a) compares the residual axial stress profiles in the FRP plate and the steel bottom flange for the NIS and WIS cases. In both cases, note that the variation of gradient of the FRP plots is consistent with the residual shear bond stress variation given in Fig. 13. For the NIS case, the FRP residual stresses are all tensile while the steel residual stresses are all compressive. Fig. 14(b) and (c) help explain why this is so. These figures show the axial stress vs external load plots for the tension steel flange and the FRP plate at each of two sections located within the plastic zone at peak load; one point at 15 mm from midspan (labeled ''Midspan'' in the plots), the other at 615 mm from midspan. Fig. 14(b) shows that nonlinearity on the steel plot for the 615 mm location, due to prior yield of the tension steel between midspan and that location, is negligible. Thus, as exemplified by Fig. 14(b) for the two locations chosen, the steel behavior within the elasto-plastic zone comprises two parallel lines separated by a yield plateau, and so the steel residual stress is always negative, or compressive. The length of the plateau, and with it the residual compressive stress, decreases as the elasto-plastic zone is traversed outwards from midspan. Fig. 14(c) shows that yield of the steel induces nonlinear upward concavity on the FRP plot, and so the unloading line always gives tensile residual stress for the FRP.

When initial self-equilibrating stresses exist in the steel member, elasto-plastic activity starts at a lower load, and this activity is more pronounced when the peak load is attained, even if this peak load of 95.6 kN/m is slightly lower than the 98.9 kN/m value for the case with no initial stresses in the steel member. It is for this reason that, as shown in Fig. 14(a), the residual tensile stresses in the FRP plate are greater for the WIS case than for the NIS case. However, for the bottom steel flange, the dominating factor is the presence of tensile stresses before the external load is applied. These initial tensile stresses shift the NIS compressive residual stress state in the bottom flange towards tensile territory; hence the solely tensile disparity between the NIS and WIS residual stress states for the steel in Fig. 14(a).

It is useful to compare the residual shear stress and axial stress profiles of Figs. 13 and 14(a) with the corresponding profiles in Figs. 8 and 9. Significant among these comparisons are the following points:

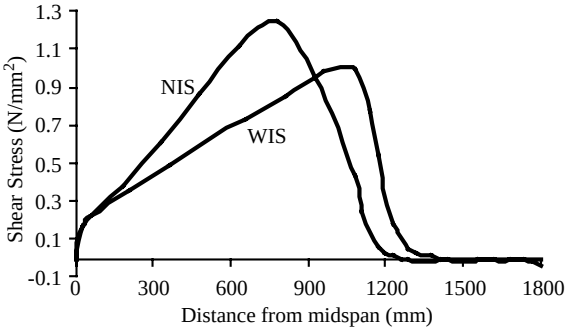

Fig. 13. Effect of initial steel stress on residual shear stress profile in adhesive.

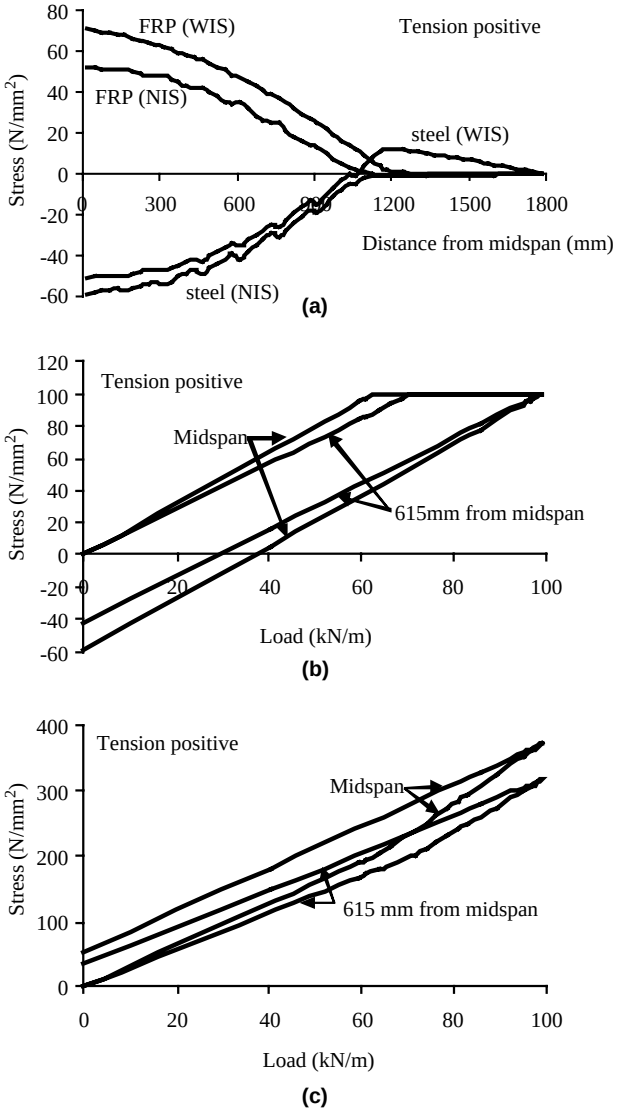

Fig. 14. Axial stresses in FRP plate and adjacent steel flange for steel yield analyses: (a) effects of initial stress in steel on residual stresses in FRP and adjacent steel; (b) axial stresses in steel tension flange for zero initial stress in steel; (c) axial stresses in FRP plate for zero initial stress in steel.

- Only forward residual shear bond stresses develop when only the steel yields, while both forward and reversed shear bond stresses occur with yield of the studs only.
- The residual shear forces on the studs are negligible (not shown) when only the steel member yields, but are high when only the studs themselves yield.
- Due to yield of the studs alone, only tensile residual stresses develop in both the FRP and tension steel flange. For yield of the steel member only, the FRP develops only tensile residual stresses, but the adjacent steel flange develops only compressive stresses if no initial self-equilibrating stresses are present in the steel member, and a mixture of compressive and tensile residual stresses if non-zero self-equilibrating stresses existed initially in the steel.

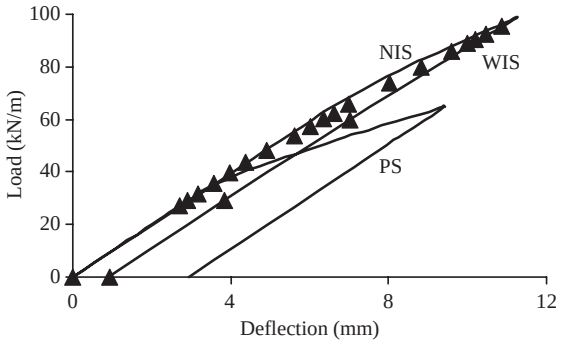

Fig. 15. Comparison of effects of stud yield and steel yield on midspan deflection.

- The peak tensile residual stress in the FRP occurs at midspan due to yield of the steel member, but occurs significantly off midspan, indeed circa 20% of the span away from midspan, due to yield of the studs.
- The residual shear and axial stresses due to steel yield are significantly higher than those due to yield of the studs only. This may well be as much a function of the relative peak loads used in the two analyses (the steel yield peak loads were almost 50% more than the stud yield peak loads) as it is a function of the effects of unit steel yield relative to unit stud yield.

In Fig. 14(a), the ripples along the steel plots and, to a lesser extent, along the FRP plots, at the locations of the studs signify sudden inputs into the steel member (and, through the adhesive, into the FRP plate) from the studs. The ripples on the FRP plots imply local fluctuations of the adhesive shear stress profile around the stud locations. This *was* observed from the FE output, but the fluctuations were removed so that smooth envelopes through the *peak* residual shear stresses could be presented as in Fig. 13. By this means, the main features of the adhesive residual shear stress distribution as discussed above were not obscured.

Finally, Fig. 15 compares the load vs midspan deflection plots for the three cases of stud yield only (PS, plasticity of studs), steel yield only NIS, and steel yield only WIS. Both the nonlinear reduction in stiffness due to yield and the residual deflection are seen to be much more significant for stud yield than for steel yield, even if the peak load for the stud yield analysis is much less than that for the steel yield analysis. Clearly, the nonlinear decrease in hybrid action due to yield of the studs is quite dramatic, while the decrease in stiffness due to steel yield is probably offset by the presence of the solely elastic FRP.

4. Further work

The preceding discussions illustrate that, in concrete–stud–steel–adhesive–FRP hybrid structures, yield of the studs generates palpably different residual stress patterns from yield of the steel member. In practice, yield of some studs may well coincide with yield of the steel, and further studies are needed to establish the nature of the resulting residual stress patterns. This work considered a single cycle of external loading. In future analyses, for different combinations of material and connection strengths, the behavior under multiple cycles of yield-inducing loads should be understood, and this understanding used to develop analytical models for path dependency in this class of structure under multiple load cases.

The implications of the build up of residual stresses for not only the ultimate limit state, but also the serviceability limit state performance of real structures of the present form, must be understood. This would assist in developing comprehensive risk-based predictions of the service lives of new and existing bridges.

This work considered a single span simply supported member. In future work, the nature of this path dependent behavior in continuous members, where the statical indeterminacy makes for more complex structural action, should be pursued.

Finally, it is seen that although yield of the studs gives somewhat more pronounced nonlinear decreases in stiffness and more pronounced residual deflection in the structure at midspan than does yield of the steel, the residual stresses due to steel yield are significantly higher than those due to stud yield. This reinforces the idea that deflection measurements alone may not necessarily give a representative idea of residual stresses locked within a structure. Such measurements should thus be combined with analytical work, if assessment of the residual stresses is a prime concern of the investigation.

5. Conclusions

FE analyses have been conducted to investigate the residual stress patterns in a single span simply supported steel beam–stud connection–concrete slab composite structure with a FRP plate adhesively-bonded to the tension flange of the steel member. Uniformly distributed loading was applied in all analyses. Three different analyses were performed; one in which only the studs yield, another in which only the steel beam yields with no initial stresses present, and a final analysis where again only the steel beam, this time with non-zero initial self-equilibrating stresses, yields. The FE results highlight the following points:

- Yield of either the studs or the steel member induces significantly nonlinear local increases of shear bond stress in the adhesive.
- Due to stud yield, both the residual adhesive shear bond stress profile and the residual stud shear force profile are significant, and both profiles entail variation from forward to reversed actions along the span. By contrast, yield of the steel beam gives negligible residual shear forces on the studs and significant, solely forward residual shear stresses in the adhesive.
- For the FRP plate, both stud yield and steel yield give solely tensile residual stresses. However, for the adjacent steel flange, while stud yield gives only tensile residual stresses, steel yield gives only compressive stresses if there are zero initial self-equilibrating stresses in the steel member, and a gradual change from compressive to tensile stresses along the member if non-zero initial self-equilibrating stresses are present.
- The maximum residual axial stress in the FRP plate occurs at midspan when yield occurs in the steel member, but circa 20% of the span off midspan when yield occurs in the studs.
- When yield occurs in the steel beam, non-zero initial self-equilibrating stresses in that beam induce earlier yield, so giving significantly increased FRP residual axial stresses and also giving a larger zone of residual stress relative to the case with no self-equilibrating stresses.
- Further work must focus on statically indeterminate structures and on developing analytical methods for path dependency in this class of structure under multiple loading patterns.
- In assessing residual stresses, analytical work must accompany deformation measurements.

References

Burgoyne, C.J. (Ed.), 2001. Proceedings FRPRCS-5 Conference, ISBN 072 77-3009-6. Thomas Telford Publishers, London.

Mertz, D., Gillespie, J., 1996. Rehabilitation of steel bridge girders through the application of advanced composite material. NCHRP 93-ID11, Transportation Research Board, Washington, DC. pp. 1–20.

Sebastian, W.M., 1996. The performance of a composite space truss bridge with glass reinforced plastic panels, PhD thesis. University of Cambridge, England.

Sebastian, W.M., 2001. Significance of midspan debonding failure in FRP-plated concrete beams. ASCE Journal of Structural Engineering 127 (7), 792–798.

Sebastian, W.M., 2002a. Sensitivities of strength and ductility of plated reinforced concrete sections to pre-existing strains. ASCE Journal of Structural Engineering 128 (5), 624–636.

Sebastian, W.M., 2002b. Prediction of interface shear stresses in elasto-plastic moment-varying zones of ACM-strengthened concrete members. ASCE Journal of Structural Engineering 128 (9), 1212–1221.

Sebastian, W.M., 2003a. Nonlinear proportionality of shear-bond stress to shear force in partially plastic regions of asymmetric FRC-laminated steel members. International Journal of Solids and Structures 40 (1), 25–46.

Sebastian, W.M., 2003b. Ductility requirements in connections of composite flexural structures. International Journal of Mechanical Sciences 45 (2), 235–251.

Sebastian, W.M., McConnel, R.E., 2000. Nonlinear FE analysis of steel–concrete composite structures. ASCE Journal of Structural Engineering 126 (6), 662–674.

Teraskiewicz, J.S., 1967. Static and fatigue behavior of simply supported and continuous beams of steel and concrete, PhD thesis. University of London, England.

Varastehpour, H., Hamelin, P., 1996. Analysis and study of failure mechanism of RC beams strengthened with FRP plate. In: Proceedings of the 2nd International Conference on Composite Materials in Bridges and Structures, Paris, vol. 1. pp. 201–211.

Yam, L.C.P., Chapman, J.C., 1972. The inelastic behaviour of continuous composite beams of steel and concrete. Proceedings of the Institution of Civil Engineers 53 (2), 487–501.